

# Two-proton removal from $^{44}\text{S}$ and the structure of $^{42}\text{Si}$

J. A. Tostevin,<sup>1,2</sup> B. A. Brown,<sup>1,3</sup> and E. C. Simpson<sup>2</sup>

<sup>1</sup>*National Superconducting Cyclotron Laboratory, Michigan State University, East Lansing, MI 48824, U.S.A.*

<sup>2</sup>*Department of Physics, Faculty of Engineering and Physical Sciences,  
University of Surrey, Guildford, Surrey GU2 7XH, United Kingdom*

<sup>3</sup>*Department of Physics and Astronomy, Michigan State University, East Lansing, MI 48824, U.S.A.*

(Dated: July 17, 2013)

Newly-published  $^{42}\text{Si}$  gamma-ray spectra and a final-state-inclusive  $^{42}\text{Si}$  production cross section value, obtained in a higher-statistics intermediate-energy two-proton removal experiment from  $^{44}\text{S}$ , are considered in terms of the final-state-exclusive cross sections computed using proposed shell-model effective interactions for nuclei near  $N = 28$ . Specifically, we give cross section predictions when using the two nucleon amplitudes of the two-proton overlaps  $\langle ^{42}\text{Si}(J^\pi) | ^{44}\text{S} \rangle$  computed using the newly-proposed SDPF-MU shell-model Hamiltonian. We show that these partial cross sections or their longitudinal momentum distributions should enable a less-tentative interpretation of the measured gamma-ray spectra and provide a more quantitative assessment of proposed shell-model Hamiltonians in this interesting and challenging region of the chart of nuclides.

PACS numbers: 24.50.+g, 25.60.-t, 25.70.-z, 27.40.+z

## I. INTRODUCTION

Measurements and theoretical predictions of the properties of the neutron-rich  $N = 28$  isotones are subjects of considerable interest and recent studies, in an attempt to understand quantitatively the role of cross-shell interactions on the erosion of the  $N = 28$  sub-shell gap – particularly for nuclei in the vicinity of  $^{42}\text{Si}$ . This interest, the major issues involved, and much of the key literature are summarised concisely in the recent Letter by Takeuchi *et al.* [1], that also reports a state-of-the-art, higher-statistics, in-flight  $\gamma$ -ray spectroscopy measurement of final states of  $^{42}\text{Si}$ . The experiment, using a fast  $^{44}\text{S}(-2p)$  two-proton removal reaction, was performed at the RIBF, RIKEN, at 210 MeV per nucleon. Accessing this region near  $Z = 14$  is a considerable experimental challenge. The region also provides new and severe challenges for theoretical calculations.

The spectrum for  $^{42}\text{Si}$  deduced in Ref. [1] was compared with the level-scheme from shell-model calculations computed from a newly-constructed  $sd - pf$  cross-shell Hamiltonian, named SDPF-MU [2]. This very recent theoretical study includes and shows very clearly the importance of the tensor-force component in the cross-shell  $sd - pf$  proton-neutron interaction for reproducing the measured  $2_1^+$ - and  $4_1^+$ -state energies and the  $B(E2, 0^+ \rightarrow 2^+)$  values in the silicon and sulfur isotopes as  $N$  approaches 28 – including the energy of the (tentatively) assigned  $^{42}\text{Si}$   $4_1^+$  state in reference [1].

The analysis of Ref. [1] tentatively assigned the observed 1431(11) keV  $\gamma$ -rays, also seen in a coincidence gate with the 742(8) keV  $\gamma$ -ray, previously identified as due to the  $2_1^+ \rightarrow 0^+$  (g.s.) transition [3], to the decay of the  $^{42}\text{Si}(4_1^+)$  state located at 2173(14) keV. The  $4_1^+$  state is at 2270 keV according to the SDPF-MU calculation. This and the other SDPF-MU bound  $^{42}\text{Si}(J^\pi)$  final states below the (somewhat uncertain) first neutron threshold, of 3.6(6) MeV [4], are collected in the first two columns

of Table I. The additional states up to 4.2 MeV are also shown. These shell-model calculations include the full  $sd$ -shell (for protons) and the full  $pf$ -shell (for neutrons) and used the code NuShellX [5]. There are candidate SDPF-MU shell-model states for each of the decay  $\gamma$ -rays observed in the inclusive spectrum of [1] since the  $4_1^+$ ,  $0_2^+$  and  $0_3^+$  shell-model states all decay through the first excited  $2_1^+$  state.

In contrast, a shell-model calculation that uses instead the SDPF-U-SI variant of the SDPF-U interaction, designed for  $0\hbar\omega$ -truncated calculations of the neutron-rich silicon isotopes in the same model space as is used here [6], produces a more fragmented spectrum with 23 sub-threshold bound  $J^\pi = 0^+, \dots, 6^+$ ,  $^{42}\text{Si}$  final states, 21 of which can be populated directly by the removal of two  $sd$ -shell protons. These states, up to a threshold energy of 3.6 MeV, are shown in Table II. Two  $1^+$  states, at 2985 and 3380 keV, that are found to have negligible direct 2p-removal cross sections are omitted from the Table, as are the predicted bound  $5^+$  (3288 keV) and  $6^+$  (3472 keV) states that cannot be populated directly. There are a further 9 excited states in the interval from 3.6 to 4.2 MeV.

In the following we calculate the cross sections for population of the individual  $^{42}\text{Si}(J^\pi)$  final states in each case, resulting from the two-proton removal reaction on a carbon target at 210 MeV per nucleon, the reaction of [1].

## II. CROSS SECTION CALCULATIONS

The removal of two like nucleons of the deficient species from highly  $N : Z$  asymmetric nuclei has: (a) been shown to proceed directly [7] and to provide spectroscopic information [8], and (b) has been assessed quantitatively using several 2p- and 2n-removal reaction test-cases on  $sd$ -shell nuclei [8, 9]. We follow the approach described in detail in these latter references. The structure details from the shell-model calculations enter the removal

reaction calculations through the two-proton overlaps, i.e.  $\Psi_{JM}^{(f)}(1, 2) = \langle 1, 2, {}^{42}\text{Si}(JM) | {}^{44}\text{S}(0^+) \rangle$ . Specifically, for each final-state,  $E_x, J$ , they generate the set of two nucleon amplitudes (TNAs)  $C_{j_1 j_2}^J$  for each active two-proton configuration in the assumed shell-model space where, for a spin  $0^+$  projectile,

$$\Psi_{JM}^{(f)}(1, 2) = \sum_{j_1 j_2} C_{j_1 j_2}^J (-1)^{J+M} / \hat{J} [\overline{\phi_{j_1}(1) \otimes \phi_{j_2}(2)}]_{J-M}.$$

Given these TNAs, the reaction is described as a sudden, direct removal process in which the removed protons interact both elastically and inelastically and reaction residues only elastically with the light nuclear target, here carbon. These absorptive two-body interactions are described by their elastic  $S$ -matrices, computed using the eikonal model from the complex residue- and proton-target optical potentials. These potentials, at 210 MeV per nucleon, were computed using the double- and single-folding models, respectively, assuming a zero-range effective nucleon-nucleon interaction based on the free pn and pp cross sections. The point nucleon density of the carbon nuclei was assumed to be of Gaussian form with a root mean squared (rms) radius of 2.32 fm. That of the  ${}^{42}\text{Si}$  residues is discussed below.

As has been detailed for a general case in Ref. [10], the following nuclear model parameters were used. (a) The point neutron and proton densities of the  ${}^{42}\text{Si}$  residues were obtained from spherical Hartree-Fock calculations using a Skyrme force (the SkX interaction [11]). The removed-proton  $sd$ -shell radial form factors were described as normalized eigenstates of a Woods-Saxon plus spin-orbit potential well whose depths were constrained by the evaluated 2p separation energy  $S_{2p} = 40.2(5)$

TABLE I: Spins, parities and excitation energies of all shell-model states below the neutron separation energy of  ${}^{42}\text{Si}$ , 3.6(6) MeV, computed using the SDPF-MU Hamiltonian of Ref. [2]. The additional states up to 4.2 MeV excitation energy are also shown. The two-proton removal partial cross sections to each final state and the inclusive cross section for states up to a 3.6 MeV threshold are also shown, calculated using the SDPF-MU TNAs.

$J^\pi$	$E_{\text{SDPF-MU}}^{SM}$ (keV)	$\sigma_{\text{th}}(-2\text{p})$ (mb)
$0_1^+$	0	0.186
$2_1^+$	821	0.031
$4_1^+$	2271	0.030
$0_2^+$	2573	0.103
$0_3^+$	3273	0.011
$2_2^+$	3525	0.012
Inclusive $\sigma_{\text{th}}(-2\text{p})$ :		0.37
$2_3^+$	3844	0.005
$3_1^+$	3899	0.007
$4_2^+$	4080	0.010
$2_4^+$	4090	0.007

TABLE II: Spins, parities and excitation energies of all  ${}^{42}\text{Si}$  shell-model states below a 3.6 MeV first neutron threshold energy having non-negligible direct two-proton removal reaction yields. The  ${}^{42}\text{Si}$  states were computed using the SDPF-U-SI interaction [6]. For the two-proton removal TNA and partial cross section calculations, the wave function for  ${}^{44}\text{S}$  was computed using the SDPF-U interaction.

$J^\pi$	$E_{\text{SDPF-U-SI}}^{SM}$ (keV)	$\sigma_{\text{th}}(-2\text{p})$ (mb)
$0_1^+$	0	0.249
$2_1^+$	815	0.025
$0_2^+$	1080	0.062
$0_3^+$	1615	0.030
$2_2^+$	1622	0.015
$4_1^+$	1792	0.028
$0_4^+$	2398	0.015
$3_1^+$	2414	0.008
$4_2^+$	2674	0.001
$2_3^+$	2709	0.013
$2_4^+$	2852	0.055
$4_3^+$	2896	0.004
$3_2^+$	3033	0.039
$2_5^+$	3222	0.006
$3_3^+$	3285	0.011
$2_6^+$	3400	0.002
$4_4^+$	3451	0.116
$2_7^+$	3563	0.008
$3_4^+$	3603	0.002
Inclusive $\sigma_{\text{th}}(-2\text{p})$ :		0.69

MeV [5] and the final state excitation energies  $E_x$ , i.e.  $S_p = (S_{2p} + E_x)/2$ . We use excitation energies  $E_x = E^{SM}$  as given by the shell-model. Fixed diffuseness (0.7 fm) and spin-orbit interaction strength (6.0 MeV) parameters were assumed throughout. The radius parameters of these Woods-Saxon binding potentials,  $r_0$ , were determined from a fit to the rms radius of each proton single-particle orbital of interest, as given by the HF-SkX calculation. These rms radii play a significant role in the determination of the removal cross sections, since they dictate the spatial extent of the two-proton position probabilities relative to the  ${}^{42}\text{Si}$  residue densities, and these two sizes must be specified consistently. Hence our usual practice of using the same theoretical (HF) model to constrain the proton radii and the densities used in the evaluation of the interaction  $S$ -matrices.

The  ${}^{42}\text{Si}$  residue longitudinal momentum distributions offer an additional signal of the spins of the populated and  $\gamma$ -decaying final-states, as has been discussed formally [12, 13] and also applied for spectroscopy; for example, in identifying the excited  $2_1^+$  and  $4_1^+$  states in  ${}^{44}\text{S}$  following the  ${}^{46}\text{Ar}(-2\text{p})$  reaction [14]. In the following section we will discuss the exclusive momentum distributions of selected SDPF-MU shell-model final states. Those

calculations use the same input parameters as have been detailed above.

### III. RESULTS

The individual final-state partial cross sections and longitudinal momentum distributions were calculated following the formalism of Refs. [8, 9] and [12, 13], respectively, from the np-form shell-model TNAs computed using NuShellX [5].

#### A. Exclusive cross sections

The calculated final-state-exclusive two-proton removal cross sections for SDPF-MU are shown in Table I, that shows the strongest populations are of the ground-state and the first excited  $0_2^+$  state. The calculated inclusive removal cross section is 0.37 mb, to be compared with the reported value of 0.15(2) mb [1]. So, the ratio of the experimental to the theoretical yields,  $R_s(2N) = \sigma_{\text{exp}}/\sigma_{\text{th}}(\text{incl.}) = 0.41(6)$ , is consistent with the systematics,  $R_s(2N) \approx 0.5$ , previously observed for a number of *sd*-shell test-case nuclei [8].

The corresponding situation, using the TNAs from the wave functions for  $^{44}\text{S}$  computed using SDPF-U and for  $^{42}\text{Si}$  computed using SDPF-U-SI, are shown in Table II. The integrated cross section to the (21) SDPF-U-SI final states is 0.69 mb. The cross section to the lowest 6 states, the  $0_{1,2,3}^+$ ,  $2_{1,2}^+$  and  $4_1^+$ , in common with the SDPF-MU bound states (though reordered), is 0.41 mb. These states all lie below 1.8 MeV when using SDPF-U-SI, indicating that significant additional strength is present at lower excitation energies and that is distributed over a large number of the additional bound final states. A very similar integrated cross section (of 0.62 mb) and pattern of final-state populations arises if instead one computes both the wave functions for  $^{44}\text{S}$  and  $^{42}\text{Si}$  using SDPF-U-SI. These calculated cross-section distributions show little correspondence with the latest experimental observations [1].

The predicted relative final-state yields of Table I on the other hand suggest clear fingerprints for a more detailed assessment of the SDPF-MU wave functions from the measured  $\gamma$ -ray yields, predicting (i) that 50% of the inclusive cross section will pass through the  $2_1^+$  state, and (ii) specific ratios for the proposed ( $4_1^+$ )-state decay strength relative to those for the  $2_1^+$ -state and the predicted excited  $0_2^+$ -state decays.

We note that prediction (i) above is consistent with the observation from the earlier lower energy and lower statistics  $^{44}\text{S}(-2p)$  measurement made at GANIL [3], which reported that 44(10)% of the reaction events were accompanied by a  $2_1^+$  to ground state transition  $\gamma$ -ray – there measured to be 770(19) keV in reasonable agreement with the new data of [1].

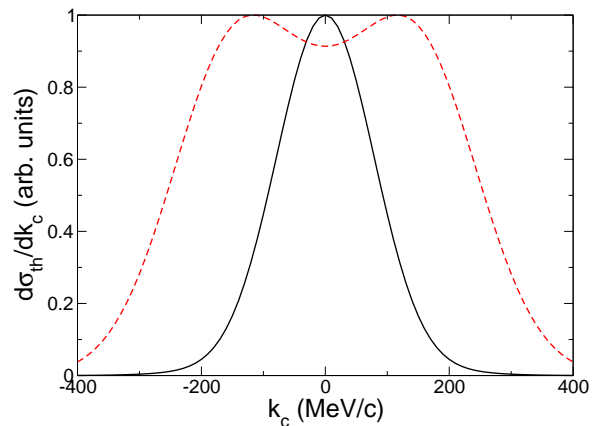


FIG. 1: (Color online) Calculated exclusive longitudinal momentum distributions in the projectile rest frame of  $^{42}\text{Si}$  residues produced in the  $0_2^+$  (solid curve) and  $4_1^+$  (dashed curve) shell-model final states of the SDPF-MU Hamiltonian [2]. These calculated momentum distributions are normalized to unity at their peaks. Their integrated cross sections were shown in Table I.

#### B. Exclusive momentum distributions

Further to the fingerprints offered by these relative partial cross sections, in Figure 1 we now show the computed exclusive longitudinal momentum distributions  $d\sigma_{\text{th}}(J^\pi)/dk_c$ , with respect to the beam-directional component of the residue momentum,  $k_c$ , in the projectile rest frame. Results are shown for  $^{42}\text{Si}$  residues produced in the  $4_1^+$  (dashed curve) and  $0_2^+$  (solid curve) SDPF-MU shell-model final states. The  $4_1^+$  state, that is dominated by the  $(d_{3/2} \otimes d_{5/2})_4$  two-proton configuration with a dominant  $L = 4$  total orbital angular momentum component, is particularly broad. This contrasts markedly with the  $0_2^+$  distribution. These large differential widths suggest that one could confirm the existence of these states from their momentum distributions in measurements with quite limited statistics.

#### C. Inclusive momentum distributions

Although less specific, the inclusive momentum distributions for (a) reactions to all final states, and (b) for all events with a coincident  $2_1^+$ -state  $\gamma$ -ray, both involving increased statistics, would also probe the SDPF-MU predictions. The predicted distributions, obtained by summing the appropriate exclusive distributions, are shown by the solid and dashed lines, respectively, in Figure 2. The predicted inclusive cross section, shown in Table I to be dominated by  $0^+$  transitions (81%), is predicted to be narrow, analogous to the solid,  $0_2^+$ -state curve shown in Fig. 1. The  $2_1^+$ -state inclusive events are predicted to be a 60 : 40% admixture of  $0^+ : (2^+ + 4^+)$  transitions. This distribution is seen to be broadened somewhat by the now 40% component from the  $2^+$ - and  $4^+$ -state distribu-

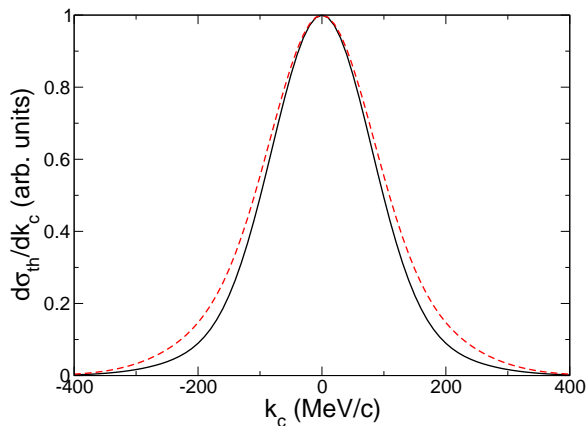


FIG. 2: (Color online) Calculated inclusive longitudinal momentum distributions in the projectile rest frame for (i) reactions to all final states (solid curve) and (ii) for all events with a coincident  $2_1^+$ -state  $\gamma$ -ray (dashed curve). Calculations use the SDPF-MU shell-model TNAs. These momentum distributions are normalized to unity at their peaks.

tions. These two distributions thus provide a valuable, but less specific profile of the predicted SDPF-MU bound states yields, in particular of the  $0^+$ -states dominance and, in the case of the coincident  $2_1^+$ -state events, the relative importance of excited  $0^+$ -states of the SDPF-MU Hamiltonian.

#### IV. SUMMARY COMMENTS

We have presented an analysis of the partial cross sections for the  $^{44}\text{S}(-2\text{p})$  two-proton removal reaction at 210 MeV per nucleon, populating the bound final states of  $^{42}\text{Si}$  predicted by the newly-developed SDPF-MU cross-shell Hamiltonian of Ref. [2]. The calculations make spe-

cific predictions for the relative populations of the final states, as were shown in Table I, that should be tested against deduced  $\gamma$ -ray yields – as should be available from the data of [1].

This could allow a considerable strengthening of the tentative assignment of a 2173(4) keV  $4_1^+$  excited state in  $^{42}\text{Si}$  made in [1] and a more detailed assessment of the predictions of the SDPF-MU Hamiltonian than can be provided by, for example, the  $2_1^+$  and  $4_1^+$  level energies. This includes the prediction of a strong population of an excited  $0_2^+$  state near 2.5 MeV. The SDPF-MU-based final-state-exclusive reaction yields presented are consistent with the earlier experimental observation [3] that 44(10)% of  $^{44}\text{S}(-2\text{p})$  reaction events were accompanied by a  $^{42}\text{Si } 2_1^+$  to ground-state decay  $\gamma$ -ray.

We also show that the computed longitudinal momentum distributions predict clear additional fingerprints of the populated final-states, with large differential widths calculated for  $^{42}\text{Si}$  residues produced in the  $4_1^+$  and  $0_2^+$  states, states that are predicted by the SDPF-MU Hamiltonian to lie at quite similar excitation energies. The inclusive momentum distributions are shown to be narrow reflecting the dominance of  $0^+$  final-state transitions predicted by the SDPF-MU Hamiltonian.

In closing we note that complementary  $^{42}\text{Si}$  final-state data from the  $^{43}\text{P}(-1\text{p})$  one-proton removal reaction would also contribute to this  $^{42}\text{Si}$  spectroscopy discussion, since  $sd$ -shell proton removal from the  $^{43}\text{P}(\frac{1}{2}^+)$  ground-state cannot directly populate proposed  $J^\pi = 4^+$ ,  $^{42}\text{Si}$  final states.

#### Acknowledgments

This work was supported by the United Kingdom Science and Technology Facilities Council (STFC) research grant ST/J000051 and by NSF grant PHY-1068217.

- 
- [1] S. Takeuchi *et al.*, Phys. Rev. Lett. **109**, 182501 (2012).  
 [2] Y. Utsuno *et al.*, Phys. Rev. C **86**, 051301(R) (2012).  
 [3] B. Bastin *et al.*, Phys. Rev. Lett. **99**, 022503 (2007).  
 [4] NuDat2, <http://www.nndc.bnl.gov/nudat2/>  
 [5] NuShellX, <http://www.garsington.eclipse.co.uk/>  
 [6] F. Nowacki and A. Poves, Phys. Rev. C **79**, 014310 (2009).  
 [7] D. Bazin *et al.*, Phys. Rev. Lett. **91**, 012501 (2003).  
 [8] J.A. Tostevin, B.A. Brown, Phys. Rev. C **74**, 064604 (2006).  
 [9] J.A. Tostevin, G. Podolyák, B.A. Brown and P.G. Hansen, Phys. Rev. C **70**, 064602 (2004).  
 [10] A. Gade *et al.*, Phys. Rev. C **77**, 044306 (2008).  
 [11] B. A. Brown, Phys. Rev. C **58**, 220 (1998).  
 [12] E. C. Simpson, J. A. Tostevin, D. Bazin, B. A. Brown, A. Gade, Phys. Rev. Lett. **102**, 132502 (2009).  
 [13] E. C. Simpson, J. A. Tostevin, D. Bazin, A. Gade, Phys. Rev. C **79**, 064621 (2009).  
 [14] D. Santiago-Gonzalez *et al.*, Phys. Rev. C **83**, 061305(R) (2011).